Biosensors and Bioelectronics 31 (2012) 137–143

Contents lists available at SciVerse ScienceDirect

Biosensors and Bioelectronics

journal homepage: www.elsevier.com/locate/bios

Monitoring extracellular K^+ flux with a valinomycin-coated silicon nanowire field-effect transistor

Ko-Shing Chang[a,b], Chih-Jung Sun[a], Pei-Ling Chiang[a,b], Ai-Chuan Chou[c], Ming-Chou Lin[d], Chieh Liang[a], Hui-Hsing Hung[c], Yu-Hsiu Yeh[a], Chii-Dong Chen[d,e], Chien-Yuan Pan[c,f,**], Yit-Tsong Chen[a,b,*]

[a] Department of Chemistry, National Taiwan University, Taipei 106, Taiwan
[b] Institute of Atomic and Molecular Sciences, Academia Sinica, P.O. Box 23-166, Taipei 106, Taiwan
[c] Institute of Zoology, National Taiwan University, Taipei 106, Taiwan
[d] Institute of Physics, Academia Sinica, Taipei, Nankang 11529, Taiwan
[e] Department of Physics, National Cheng Kung University, Tainan 701, Taiwan
[f] Department of Life Science, National Taiwan University, Taipei 106, Taiwan

ARTICLE INFO

Article history:
Received 29 July 2011
Received in revised form 2 October 2011
Accepted 5 October 2011
Available online 12 October 2011

Keywords:
Field-effect transistor
Nanowire
Nicotinic acetylcholine receptor
Potassium efflux
Valinomycin

ABSTRACT

A silicon nanowire field-effect transistor (SiNW-FET) coated with a polyvinyl chloride (PVC) membrane containing valinomycin (VAL) was employed as a biosensor (referred to as VAL-PVC/SiNW-FET) to detect the K^+-efflux from live chromaffin cells. The detection sensitivity of K^+ with the VAL-PVC/SiNW-FET covers a broad range of concentrations from 10^{-6} to 10^{-2} M. The apparent association constants between VAL and Li^+, Na^+, K^+, and Cs^+ in Tris buffer solution were determined to be 67 ± 42, 120 ± 23, 5974 ± 115, and $4121 \pm 140\ M^{-1}$, respectively. By culturing chromaffin cells on the VAL-PVC/SiNW-FET, the conductance was significantly increased by nicotine stimulation in a bath buffer without Na^+. The K^+ concentration at the cell surface was determined to be ~20 μM under the stimulation of 5 mM nicotine. These results demonstrate that the VAL-PVC/SiNW-FET is sensitive and selective to detect the released K^+ from cells and is suitable for applications in cellular recording investigations.

1. Introduction

The asymmetric distribution of various ions across the plasma membrane is an important physiological property of live cells. The two main mechanisms responsible for the differences in ionic concentrations across the plasma membrane are the impermeability of the plasma membrane to charged molecules and the Na^+/K^+-ATPases residing within the plasma membrane. The Na^+/K^+-ATPase transports three Na^+ ions out of and two K^+ ions into the cell with the consumption of one equivalent of ATP, resulting in a concentration gradient of K^+ and Na^+ across the membrane (Glitsch, 2001). A slight efflux of K^+ is essential for the resting membrane potential. When cells are excited, the quick consecutive openings of voltage-gated Na^+ and K^+ channels constitute an action potential for signal transduction. Abnormalities in K^+ permeability have been suggested to be involved in diseases like epilepsy, diabetes mellitus, and neural degeneration (Jentsch, 2000; MacDonald et al., 2001; Singh et al., 1998). Accordingly, the importance of K^+ flux across the plasma membrane of a cell to regulate its normal physiological activities cannot be underestimated. Therefore, the measurements of cellular K^+ flux to monitor the ions' effect in modulating the membrane potential are of fundamental significance to the understanding of neural excitability.

In addition to the voltage-gated ion channels, the excitatory ionotropic neurotransmitter receptors at postsynaptic synapses can respond to the released neurotransmitters and allow the flux of Na^+, K^+, and Ca^{2+} through their conjugated channels. According to the electrochemical gradient, K^+ moves outward, while Na^+ and Ca^{2+} move inward to depolarize the membrane potential, which then propagates to the soma for signal integration to determine the initiation of an action potential (Barnett and Larkman, 2007). Adrenal medulla cells, differentiated from the sympathetic postganglionic neurons, have nicotinic-type acetylcholine receptors

Abbreviations: ACh, acetylcholine; BOX, buried oxide; C_{K^+}, K^+ concentration; C_{M^+}, metal ion concentration; $C_{nicotine}$, nicotine concentration; G, electrical conductance; ΔG, conductance change; HB, hexamethonium bromide; I_{sd}, source-drain current; K_a, association constant; M^+, alkali metal ion; nAChR, nicotinic-type acetylcholine receptor; NMG, N-methyl-D-glucamine; PDMS, polydimethylsiloxane; PLL, poly-L-lysine; PVC, polyvinyl chloride; SEM, scanning electron microscopy; SiNW-FET, silicon nanowire field-effect transistor; SOI, silicon-on-insulator; Tris, tris(hydroxymethyl)aminomethane; VAL, valinomycin; V_g, backgate voltage; V_{sd}, source-drain voltage.

* Corresponding author at: Department of Chemistry, National Taiwan University, Taipei 106, Taiwan. Tel.: +886 2 33668198; fax: +886 2 23636359.
** Corresponding author at: Institute of Zoology, National Taiwan University, Taipei 106, Taiwan. Tel.: +886 2 33662452; fax: +886 2 23636837.
E-mail addresses: cypan@ntu.edu.tw (C.-Y. Pan), ytcchem@ntu.edu.tw (Y.-T. Chen).

0956-5663/$ – see front matter © 2011 Elsevier B.V. All rights reserved.
doi:10.1016/j.bios.2011.10.005

(nAChRs) at the plasma membrane that can respond to the acetylcholine (ACh) released from sympathetic neurons. Upon agonist binding, the nAChR nonselective ion channels allow the net flow of positively charged ions inward to depolarize the membrane potential (Sala et al., 2008). Subsequently, the depolarization will open the voltage-gated Na^+ channels to further depolarize the membrane potential and then activate the voltage-gated Ca^{2+} channels to elevate the intracellular Ca^{2+} concentration for catecholamine release (Barrantes et al., 1995; Dani and Bertrand, 2007). However, if there is no extracellular Na^+, the membrane potential would not be elevated to a level high enough for the activation of other voltage-gated ion channels; meanwhile, only K^+ and Ca^{2+} will move across the nAChR.

To characterize the ion flux across the plasma membrane, electrophysiological recording that can provide the detailed kinetics of ion currents is the most direct technique to monitor the activities of ion channels. However, recording is time-consuming, needs specialized equipment, and requires special skills. In addition, electrophysiological recording measures the net flux of all ions, rather than just one particular ion. Specific ion-sensitive fluorescence dyes have been developed to monitor the concentration of ions like Na^+ and Ca^{2+} in the cytosol (Xu et al., 2001). However, the efflux of K^+ from a cell and its subsequent effect on neighboring cells has not yet been well characterized.

Effluxed K^+ ions diffuse quickly away from the cultured cell; in contrast, effluxed K^+ ions will accumulate at the cell–cell interface in tissue and elevate the local concentration of K^+ (denoted by C_{K^+}). Such elevation in C_{K^+} may affect the membrane potential and excitability of nearby cells (Bostock and Grafe, 1985). Therefore, the K^+ efflux from a cell not only repolarizes its own membrane potential but also regulates the excitability of neighboring cells. When a certain number of neurons fire together, as in epilepsy, the effect is amplified despite this effect being distance-limited. As a consequence, the C_{K^+} on the membrane surface is an important issue in neurotransmission and needs to be investigated.

Over the past two decades, nanomaterials such as quantum dots (Raymo and Yildiz, 2007), nanoparticles (Rosi and Mirkin, 2005; Tansil and Gao, 2006), nanowires (Cui et al., 2001), nanotubes (Star et al., 2003; Tsai et al., 2008; Wang et al., 2007), nanogaps (Liang and Chou, 2008), and nanoscale films (Shan et al., 2009) have received enormous attention because of their suitable properties for designing novel nanoscale sensors. For instance, the dimension of nanomaterials at 1–100 nm provides a perfect feature to study most biological entities (Curreli et al., 2008), such as nucleic acids, proteins, viruses, and cells. In addition, the high surface-to-volume ratios of nanomaterials allow a huge proportion of the constituent atoms to be located at or near the material surface. This characteristic makes the surface atoms play an extremely important role in determining the physical, chemical, and electronic properties of nanomaterials. Compared with devices made of micrometer-sized or bulk materials, nanomaterial-configured sensors commonly possess much better sensitivity, which is closely related to the reduced dimensionality and large surface-to-volume ratio. In general, nanoscale sensors have the advantages of high sensitivity, specificity, high-speed sample delivery, fast response time, and the requirement of only trace amounts of analyte (Chen et al., 2011). To date, nanoscale sensors have found a plethora of applications in many areas of the life sciences, clinical tests, and small molecule analysis (Chen et al., 2011).

Among nanoscale sensors, silicon nanowire field-effect transistors (SiNW-FETs) have been demonstrated to be a powerful molecular recognition-sensing platform for detecting proteins (Lin et al., 2009, 2010; Pui et al., 2011), DNA sequences (Bunimovich et al., 2006; Li et al., 2004), small molecules (Chang et al., 2009; Mcalpine et al., 2008), cancer biomarkers (Lee et al., 2009; Zheng et al., 2005), viruses (Patolsky et al., 2004), and cells (Huang et al., 2011; Patolsky et al., 2006; Stern et al., 2008; Tian et al., 2010). Despite the successful detections of a myriad of biomolecules by SiNW-FET, there are few examples of the employment of SiNW-FETs for probing biological metal ions. Several traditional methods, such as potentiometry and photometry (Lin et al., 2002; Meuwis et al., 1995; Nagatoishi et al., 2005; Pandey and Prakash, 1998), were reported previously for K^+ detection; however, the low sensitivity and/or poor selectivity over other metal ions (e.g., Na^+ and Li^+) have hindered the wide applications of these conventional methods for biological investigations. Notably, some micrometer-sized FETs were used previously for the investigation of the C_{K^+} released from live neurons and HEK 293 cells (Ingebrandt et al., 2005; Vassanelli and Fromherz, 1999; Wrobel et al., 2005); however, the employed FET devices were not modified with a specific receptor of high selectivity for K^+.

In this study, a nanoscale sensor for probing K^+ has been constructed by integrating valinomycin molecules ($C_{54}H_{90}N_6O_{18}$, abbreviated as VAL) with polyvinyl chloride (PVC) membrane onto a SiNW-FET surface (referred to as VAL-PVC/SiNW-FET, as illustrated schematically in Fig. 1(a)). The VAL molecule, a dodecadepsipeptide synthesized by several *Streptomyces* strains, has a high affinity for K^+ relative to other alkali metal ions like Na^+ (Lavinia et al., 1969; Eyal and Rechnitz, 1971; Rose and Henkens, 1974). The VAL-PVC/SiNW-FET responded differentially to various alkali metal ions (M^+) of Li^+, Na^+, K^+, and Cs^+ with concentrations ranging from 10 mM to the best detection limit of 1 μM. To test the effectiveness of the VAL-PVC/SiNW-FET in detecting K^+ efflux from single cells, bovine chromaffin cells were seeded on a device chip as illustrated in Fig. 1(b). When nicotine was applied to activate the nAChR and induce K^+ efflux, the electrical conductance (G, units in siemen (S)) of VAL-PVC/SiNW-FET increased as well. Our results reveal that VAL-PVC/SiNW-FET is able to discriminate various effluxed C_{K^+} from live cells, thus providing a useful platform to monitor the C_{K^+} in biological samples.

2. Materials and methods

2.1. Chemicals

Bis(1-butylpentyl) adipate, PVC, and potassium tetrakis(4-chlorophenyl) borate were purchased from Fluka. Tris(hydroxymethyl)aminomethane (abbreviated as Tris), VAL, and all other chemicals were reagent grade from Sigma–Aldrich. Dulbecco's modified Eagle's medium and all other reagents for cell culture were purchased from Invitrogen.

2.2. Fabrication of SiNW-FET devices

SiNW-FETs were fabricated from silicon-on-insulator (SOI) wafers as described in previous publications (Chen et al., 2011; Li et al., 2004; Lin et al., 2007). SOI wafers offer a layer of high quality single-crystal silicon (referred to as the "device layer") separated from the bulk substrates by a layer of buried oxide (abbreviated as the "BOX layer"). The SOI wafers are presently state-of-the-art in metal-oxide-semiconductor field-effect-transistors (MOSFETs) in the mainstream semiconductor industry. In this work, four-inch n-type SOI wafers containing a 50-nm-thick device layer and a 400-nm-thick BOX layer were used, in which the resistivity of the device layer was approximately 100 Ω cm (where the phosphor-doping concentration was 4×10^{19} cm^{-3}). After fabrication following standard electron-beam lithographic and photolithographic procedures, the SiNWs were thermally oxidized to form a SiO_2 insulating layer to prevent both the charge transfer between SiNW-FET and analyte molecules and the electrical leaking in the subsequent sensing measurements in aqueous

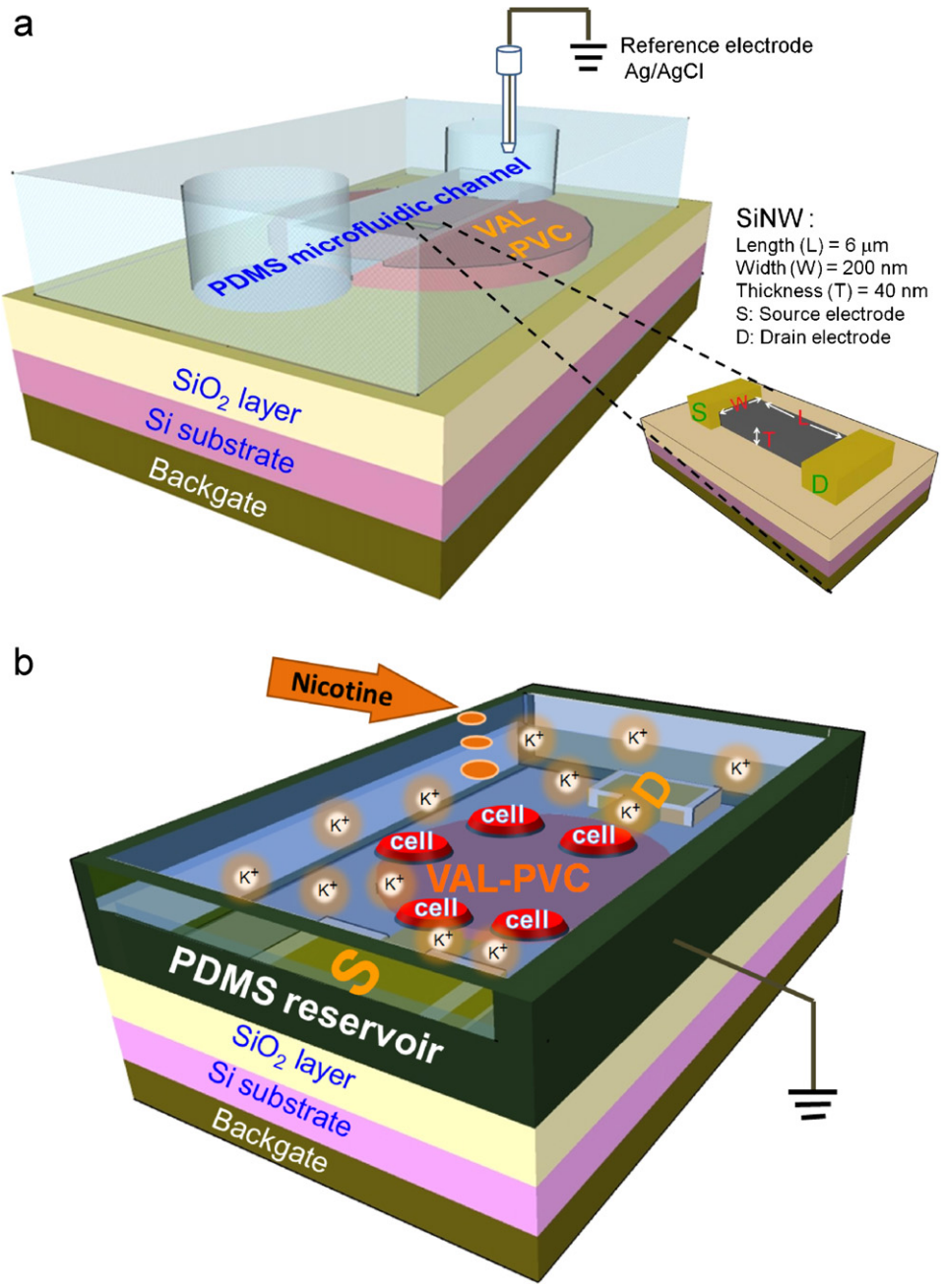

Fig. 1. Schematic illustrations for the experimental setups. (a) A PVC membrane containing VAL molecules was coated on the SiNW-FET device arrays to form a VAL-PVC/SiNW-FET. In the C_{M^+}-dependent measurements to determine the K_a values of VAL to various alkali metal ions (M^+), a PDMS microfluidic channel (6.25 mm × 0.5 mm × 0.05 mm) was designed to couple the SiNW-FET arrays to guide the flow of the sample solution. An Ag/AgCl electrode was used as a solution gate and was kept at ground potential in electrical measurements. (b) In the cell experiments, a PDMS reservoir (8 mm × 5 mm × 5 mm) was glued onto the SOI chip to hold NMG buffer. Live chromaffin cells seeded on the PLL-coated VAL-PVC/SiNW-FET device arrays were stimulated with nicotine to release K^+ ions.

solution. The chip is 14 mm × 14 mm in size and each chip contained eight SiNW-FETs. The contact pads (Ni/Au = 10 nm/50 nm) made by photolithography were attached directly to the Si device layers. The backside of the chip was coated with a metal film (Ni/Au = 15 nm/65 nm), which served as a backgate electrode. A scanning electron microscopy (SEM) image of the as-fabricated SiNW-FET devices is shown in Fig. S1(a) of Supplementary data. Typical source-drain current vs. backgate voltage (I_{sd}–V_g) curves of the SiNW-FET device are presented in Fig. S1(b) and (c).

2.3. Preparation of VAL-PVC membrane

For detecting K^+, SiNW-FETs were coated with a VAL-PVC membrane to form a VAL-PVC/SiNW-FET. This ion-selective VAL-PVC membrane was prepared by dissolving 5 mg VAL, 1.1 mg potassium tetrakis(4-chlorophenyl) borate, 24.4 μL bis(1-butylpentyl) adipate, and 11 mg PVC (m.w. ~1×10^6 g/mol) in 200 μL of 3:1 cyclohexanone/tetrahydrofuran (Cid et al., 2008). To coat the SiNW, 5 μL VAL-PVC mixture was dropped onto the chip (14 mm × 14 mm) and air-dried. The thickness of a typical VAL-PVC membrane was measured to be 8.4 ± 1.1 μm with a profilometer (XP-100, Ambios Technology).

2.4. Electrical measurement

The G of VAL-PVC/SiNW-FET was measured using a lock-in amplifier (Stanford Research System, SR830) operated at a modulation frequency of 79 Hz with a time constant of 100 ms. The

devices were biased with a source-drain voltage (V_{sd}) of 30 mV and V_g was set to zero. An Ag/AgCl electrode (BAS, MF2052) coupled to the PDMS microfluidic channel was used as a solution gate (Fig. 1(a)) and kept at ground potential throughout the real-time electrical measurements to minimize noise in the system. In the detection of M^+, different C_{M^+} in Tris buffer (100 mM Tris-acetate at pH 6.5) was flown at 500 μL/h through a polydimethylsiloxane (PDMS) microfluidic channel (6.25 mm × 0.5 mm × 0.05 mm), which was coupled with the SiNW-FET arrays (as illustrated in Fig. 1(a)). After each detection, the alkali ions that associated with VAL could be washed off by flushing Tris buffer through the PDMS microfluidic channel at 500 μL/h for 1 h to return the surface of VAL-PVC/SiNW-FET to its original state.

2.5. Chromaffin cell culture

Bovine adrenal medulla chromaffin cells were isolated and cultured as described before (Pan et al., 2006). The VAL-PVC/SiNW-FET device was coated with poly-L-ysine (PLL) and seeded with $\sim 1 \times 10^6$ chromaffin cells. Cells were cultured in Dulbecco's modified Eagle's medium supplemented with 10% fetal bovine serum and maintained in a water-saturated incubator under an atmosphere of 5% CO_2 and 95% air at 37 °C for three days. For chemical stimulation, the cells were washed and incubated in N-methyl-D-glucamine (NMG) buffer (135 mM NMG, 5 mM glucose, 10 mM HEPES (4-(2-hydroxyethyl)-1-piperazineethanesulfonic acid), 1 mM $MgCl_2$, and 2.2 mM $CaCl_2$, pH 7.3). Nicotine was dissolved in NMG buffer and added into the recording chamber.

For electrophysiology recording, cells in NMG buffer were whole-cell patched with a pipette solution (130 mM K-aspartate, 20 mM KCl, 1 mM $MgCl_2$, 0.1 mM EGTA, 3 mM Na_2ATP, 0.1 mM Na_2GTP, and 20 mM HEPES at pH 7.3.) as described previously (Pan et al., 2007). Cells were first tested under voltage-clamp mode to record the nicotine-induced current and then switched to current-clamp mode for the membrane potential measurement.

3. Results and discussion

To test the sensitivity of VAL-PVC/SiNW-FET in detecting M^+, Tris buffer containing various C_{M^+} was pumped through a PDMS microfluidic channel coupled with the SiNW-FET arrays (Fig. 1(a)). In the electrical measurements, the dissolution of M^+ in Tris buffer was to keep the total ionic strength of the sample solution constant, which could prevent the unnecessary conductance change (ΔG) of VAL-PVC/SiNW-FET from varying analyte solutions of different C_{M^+}. As displayed in Fig. 2(a)–(d), the increase in G of VAL-PVC/SiNW-FET with elevating C_{M^+} denotes that the employed SiNW-FET is an n-type semiconductive sensor. The ΔG was small for Li^+ and Na^+ at $\leq 10^{-3}$ M, while the ΔG was still significant for K^+ and Cs^+ even at 10^{-6} M. The relative ΔG of VAL-PVC/SiNW-FET is defined as $\Delta G\% = (G - G_0) \times 100/G_0\%$, where G_0 is the conductance level at a low C_{M^+} that induces no detectable signals. Fig. 2(e) summarizes the measured data of $\Delta G\%$ vs. C_{M^+} for Li^+, Na^+, K^+, and Cs^+. At $C_{M^+} = 10$ mM, the $\Delta G\%$ was 4.95 ± 0.33 and $5.68 \pm 0.68\%$ for Cs^+ and K^+, respectively, while it was only 0.32 ± 0.08 and $0.48 \pm 0.13\%$ for Na^+ and Li^+, respectively. These results indicate that the VAL-PVC/SiNW-FET has distinctive binding affinities against various C_{M^+}.

The apparent association constants (K_a) of VAL to M^+ were determined by the Langmuir adsorption isotherm model (Ohno et al., 2009): $C_{M^+}/\Delta G = (1/\Delta G_{max}) \cdot C_{M^+} + 1/(\Delta G_{max} \cdot K_a)$, where ΔG_{max} is the saturated ΔG at high C_{M^+}. Fig. 2(f) shows that, by plotting $C_{M^+}/\Delta G$ against C_{M^+} the K_a values could be determined by a least-squares fit to be 67 ± 42, 120 ± 23, 5974 ± 115, and $4121 \pm 140\ M^{-1}$ for Li^+, Na^+, K^+, and Cs^+, respectively. The M^+ needs to be dehydrated before binding to the central cavity of VAL, where the association stabilizes the M^+–VAL complex (Steed and Atood, 2000; Varma et al., 2008); therefore, the K_a is affected by the solution used. Table 1 summarizes the K_a values of the VAL–K^+ complex in isopropanol, methanol, and water determined from several earlier measurements and in this study (Ehala et al., 2008; Izatt et al., 1985; Rose and Henkens, 1974). In methanol, the K_a of VAL for K^+ was reported to be $\sim 10^4$–$10^5\ M^{-1}$, approximately one order of magnitude larger than the value obtained in this experiment. In this work, because VAL was embedded in the PVC layer and K^+ was dissolved in Tris buffer, the high dielectric constant of the polar solvent (i.e., water) stabilized the solvated K^+ complex and lowered the binding affinity of K^+ to VAL (Varma et al., 2008). In addition, since the VAL–K^+ complexes were embedded in the PVC layer, the electric filed exerted from the captured K^+ ions to induce SiNW-FET signals could be partially shielded by the PVC membrane. These factors may explain why the binding of VAL and K^+ was weaker in this experiment than what had been reported previously.

It was estimated that only those captured K^+ ions within the region of about ~10 nm to the SiNW surface could effectively induce ΔG signals in the VAL-PVC/SiNW-FET (Chen et al., 2011). Fig. S2 shows that, in the electrical measurement using a VAL-PVC/SiNW-FET, the signal response time as well as the amplitude of ΔG show no strong dependence on the thickness of the VAL-PVC membranes, suggesting that K^+ ions could diffuse in the PVC membrane. However, the thick VAL-PVC layer (~8 μm) could have reduced the detection sensitivity of VAL-PVC/SiNW-FET, since K^+ ions could associate with VAL before arriving at the effective region near the SiNW surface to induce ΔG signals. Seeking a thin membrane to accommodate VAL on the SiNW-FET surface to prevent this detrimental sample consumption is called for in the future study.

To examine the growth of chromaffin cells on the device, live chromaffin cells were stained with FM4-64, a plasma membrane-staining fluorescent dye, and visualized by fluorescent microscope (Fig. 3(a)). Cells were located randomly on the FET device surface coated with PLL but not on the chip without PLL coating. These data suggest that the VAL-PVC/SiNW-FET devices could support the growth of chromaffin cells for K^+ measurement.

To verify the capability of VAL-PVC/SiNW-FET in detecting the release of K^+ from live cells, chromaffin cells was stimulated with nicotine in NMG buffer (Fig. 3(b)). The activation of nAChR by nicotine will open its conjugated ion channel and allow the flux of Na^+ and Ca^{2+} into and K^+ out of the cell under normal physiological conditions. To detect the efflux of K^+ by VAL-PVC/SiNW-FET without the competition of Na^+ in VAL binding, NMG was used to replace the external Na^+ in the extracellular bath buffer. The G of chromaffin cell-seeded VAL-PVC/SiNW-FET was increased and remained at a constant level in response to elevated concentrations of nicotine ($C_{nicotine}$). Before cell seeding, the ΔG of the same VAL-PVC/SiNW-FET device was calibrated with different C_{K^+} from 10^{-6} to 10^{-1} M (Fig. S3). According to this calibrated response curve, the ΔG obtained from Fig. 3(b) was converted to C_{K^+} as a function of $C_{nicotine}$ (Fig. 3(c)). The C_{K^+} was gradually elevated to a plateau of approximately 20 μM when $C_{nicotine}$ reached 5 mM. The obtained sigmoidal concentration–response curve indicates a positive cooperative nicotine-induced responses. The G increment was not due to the positively charged nicotine; as shown in Fig. S4, the addition of nicotine up to 5 mM onto the VAL-PVC/SiNW-FET device without chromaffin cell adhesion did not induce any significant ΔG. These results suggest that the VAL-PVC/SiNW-FET can sense the K^+ efflux through the activated nAChRs in chromaffin cells.

PLL is a positively charged polymer at neutral pH with a molecular weight ranging from 70 to 150 kDa. The surface charge of a PLL-modified TiO_2 surface was reported to be 5 μC/cm^2 (Kenausis et al., 2000), equivalent to 0.3 charge/nm^2. The VAL-PVC/SiNW-FET

Table 1
The K_a values of VAL–K^+ binding determined with different methods in various solvents.

Medium	Dielectric constant	Method	log K_a	Reference
Isopropanol	20	Spectrophotometry	7.5	Rose and Henkens (1974)
Methanol	33	Potentiometry	>3.9	Izatt et al. (1985)
		Electric conductivity	4.43, 3.96	Izatt et al. (1985) and Ehala et al. (2008)
		Fluorescence spectra	4.79	Izatt et al. (1985)
		Spectrophotometry	4.9	Izatt et al. (1985)
Water	80	SiNW-FET	3.78	This study

might have introduced a barrier for K^+ (1.3 Å in radius) to approach the PVC layer, causing an underestimation of the K^+ efflux from the cells. However, Fig. S5 shows that there was no apparent difference in the G induced by the same C_{K^+} on a SiNW-FET with or without PLL coating. It is speculated that the surface charge caused by PLL coating on the hydrophobic PVC surface is much less than that on the hydrophilic TiO_2, but still enough for cell attachment.

To verify that the ΔG in Fig. 3(b) was caused by the opening of nAChRs, chromaffin cells were treated with hexamethonium bromide (HB) before nicotine stimulation (Fig. 4). HB is a quaternary ammonium ion and has been suggested to work as an open channel blocker for nAChR (Nooney et al., 1992; Xiao et al., 1998). As demonstrated in Fig. 4(a), the G response caused by nicotine (3 mM) was suppressed in the presence of 10 nM (red curve) and 100 μM HB (blue curve). Fig. 4(b) shows that the averaged normalized relative ΔG were 84 ± 5 and 64 ± 4% in the presence of 10 nM (red column) and 100 μM HB (blue column), respectively. It has been shown that HB is less effective in blocking K^+ diffusion out of the cell through the nAChR. In addition, the $C_{nicotine}$ used was much higher than the C_{HB} applied; therefore, HB might not inhibit all of the K^+ efflux. The decrease in the G response is not due to the application of positively charged HB because the inhibitory effect of 1 mM HB (not shown) is similar to that of 100 μM. These results indicate that the activation of nAChRs is responsible for the nicotine-induced increase of G in the VAL-PVC/SiNW-FET.

Under normal physiological conditions, due to the negative resting membrane potential, the activation of nAChRs mainly allows the influx of Na^+ and depolarizes the membrane potential to activate other voltage-gated Na^+ and K^+ channels for action potential generation. The replacement of the extracellular Na^+ with NMG eliminated the competition of Na^+ with K^+ in binding VAL, the efflux of K^+ was limited due to the negative membrane potential (Fig. S6). On the other hand, the influx of Ca^{2+} through the activated nAChR induced a small transient depolarization and enhanced the K^+ efflux. The K^+ efflux then hyperpolarized the membrane potential toward the reversal potential of K^+ and hindered the K^+ from

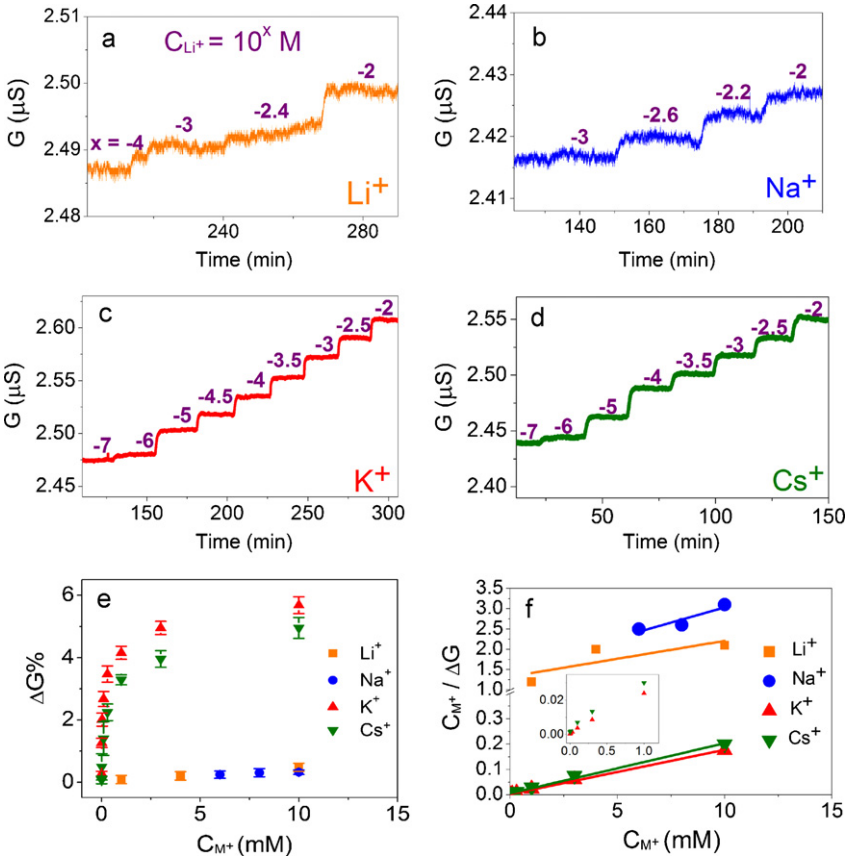

Fig. 2. Differential responses of VAL-PVC/SiNW-FET to various monovalent cations. (a)–(d) The G of a VAL-PVC/SiNW-FET was measured as a function of various C_{M^+} for the determination of K_a of VAL to M^+ = Li^+, Na^+, K^+, and Cs^+, respectively. The C_{M^+} (units in M) is expressed by the power to base 10 symbolized with the labeled number. (e) A summary of the normalized ΔG% values measured as a function of C_{M^+} (units in mM). (f) The $C_{M^+}/\Delta G$ vs. C_{M^+} (units in mM) plots for Li^+ (orange), Na^+ (blue), K^+ (red), and Cs^+ (green). Inset shows an expanded scale at $C_{M^+} < 1$ mM for the measured K^+ (red) and Cs^+ (green) data points. These measured data were used to determine the K_a of VAL–M^+ binding by least-squares fitting to the Langmuir adsorption isotherm model. (For interpretation of the references to color in this figure legend, the reader is referred to the web version of this article.)

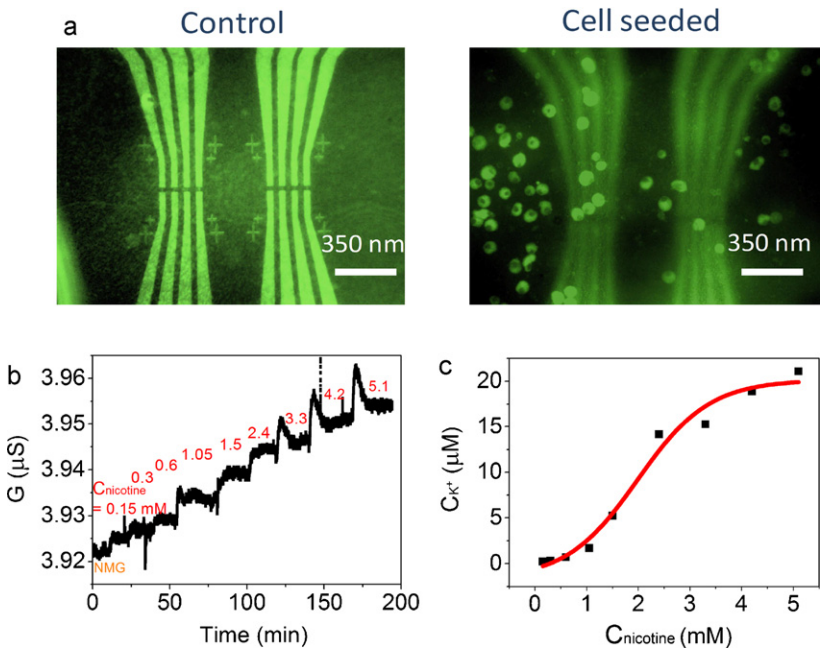

Fig. 3. Nicotine-induced K^+ release from chromaffin cells. (a) Fluorescence images of (left) a blank SOI chip consisting of eight SiNW-FET arrays and (right) stained chromaffin cells with a cellular membrane staining dye of FM4-64 seeded on the SiNW-FET arrays. (b) A chromaffin cell-seeded VAL-PVC/SiNW-FET responds to the released K^+ under various doses of nicotine stimulation with the extracellular Na^+ being replaced by NMG buffer. The labeled numbers represent the added $C_{nicotine}$ (units in mM). The increasing G reflects that more K^+ efflux was induced when more nicotine was added to activate the nAChR nonselective ion channels. (c) A plot to summarize the K^+ efflux (C_{K^+}) as a function of different doses of nicotine stimulation.

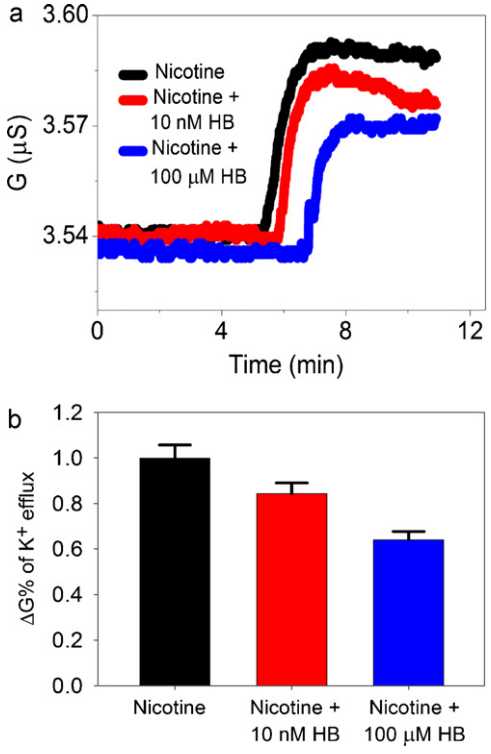

Fig. 4. HB inhibits nicotine-induced conductance change. (a) The net G was measured from the inhibited nAChRs of the nicotine-stimulated chromaffin cells. The decrease in G is attributed to the reduced K^+ efflux from the nAChR nonselective ion channels, resulting from the pretreatment of HB to block the function of nAChR. (b) The inhibition levels caused by HB were estimated from the $\Delta G\%$ to calculate the effluxed C_{K^+}. After the additions of 10 nM and 100 μM of HB, the C_{K^+} accumulated in NMG buffer remained at $84 \pm 5\%$ and $64 \pm 4\%$, respectively.

diffusing out of the cell. Therefore, little K^+ left the cell through the nAChRs in the absence of Na^+, and the extracellular K^+ could only be slightly elevated. Nevertheless, the VAL-PVC/SiNW-FET was sensitive enough to monitor the *in situ* release of K^+ from stimulated chromaffin cells.

4. Conclusions

In summary, we have successfully integrated VAL with SiNW-FET to detect the effluxed K^+ from live chromaffin cells. The detection sensitivity of VAL-PVC/SiNW-FET covers a broad range of concentrations from 10^{-6} to 10^{-2} M, suggesting that this sensorial device is appropriate for biological applications under normal physiological conditions. Although the K_a of VAL dissolved in PVC is lower in aqueous solution than that reported using methanol as a solvent, the relative order in the binding affinity of VAL to various M^+ is the same: $K^+ \sim Cs^+ > Na^+ \sim Li^+$. In the measurement of K^+-efflux from the nicotine-stimulated chromaffin cells in NMG buffer, despite little effluxed K^+ due to the incapability of chromaffin cells in depolarization, the VAL-PVC/SiNW-FET still showed a sensitive response to the released K^+. With such sensitive and selective K^+ detection, this VAL-PVC/SiNW-FET device is suitable for applications in cellular recording investigations.

Acknowledgments

This work is supported in part by the National Science Council of Taiwan, ROC under Grant Nos. NSC 99-2627-M-002-001, NSC 99-2627-M-001-001, and NSC 99-2627-M-002-002. Technical support from NanoCore, the Core Facilities for Nanoscience and Nanotechnology at Academia Sinica, is acknowledged.

Appendix A. Supplementary data

Supplementary data associated with this article can be found, in the online version, at doi:10.1016/j.bios.2011.10.005.

References

Barrantes, G.E., Murphy, C.T., Westwick, J., Wonnacott, S., 1995. Neurosci. Lett. 196, 101–104.
Barnett, M.W., Larkman, P.M., 2007. Pract. Neurol. 7, 192–197.
Bostock, H., Grafe, P., 1985. J. Physiol. 365, 239–257.
Bunimovich, Y.L., Young, S.S., Yeo, W.-S., Amori, M., Kwong, G., Heath, J.R., 2006. J. Am. Chem. Soc. 128, 16323–16331.
Chang, K.S., Chen, C.C., Sheu, J.T., Li, Y.-K., 2009. Sens. Actuators B 138, 148–153.
Chen, K.-I., Li, B.-R., Chen, Y.T., 2011. Nano Today 6, 131–154.
Cid, C.C., Riu, J., Maroto, A., Rius, F.X., 2008. Analyst 133, 1001–1004.
Cui, Y., Wei, Q., Park, H., Lieber, C.M., 2001. Science 293, 1289–1292.
Curreli, M., Zhang, R., Ishikawa, F.N., Chang, H.K., Cote, R.J., Zhou, C., Thompson, M.E., 2008. IEEE Trans. Nanotechnol. 7, 651–667.
Dani, J.A., Bertrand, D., 2007. Annu. Rev. Pharmacol. Toxicol. 47, 699–729.
Ehala, S., Kasicka, V., Makrlik, E., 2008. Electrophoresis 29, 652–657.
Eyal, E., Rechnitz, G.A., 1971. Anal. Chem. 43, 1090–1093.
Glitsch, H.G., 2001. Physiol. Rev. 81, 1791–1826.
Huang, Y., Cai, D., Chen, P., 2011. Anal. Chem. 83, 4393–4406.
Ingebrandt, S., Yeung, C.-K., Krause, M., Offenhausser, A., 2005. Eur. Biophys. J. 34, 144–154.
Izatt, R.M., Bradshaw, J.S., Nielsen, S.A., Lamb, J.D., Christensen, J.J., 1985. Chem. Rev. 85, 271–339.
Jentsch, T.J., 2000. Nat. Rev. Neurosci. 1, 21–30.
Kenausis, G.L., Voros, J., Elbert, D.L., Huang, N., Hofer, R., Ruiz-Taylor, L., Textor, M., Hubbell, J.A., Spencer, N.D., 2000. J. Phys. Chem. B 104, 3298–3309.
Lavinia, A.R., Pioda, V., Simon, W., 1969. Anal. Lett. 2, 665–674.
Lee, H.-S., Kim, K.S., Kim, C.-J., Hahn, S.K., Jo, M.-H., 2009. Biosens. Bioelectron. 24, 1801–1805.
Li, Z., Chen, Y., Li, X., Kamins, I., Nauka, K., Williams, R.S., 2004. Nano Lett. 4, 245–247.
Liang, X.G., Chou, S.Y., 2008. Nano Lett. 8, 1472–1476.
Lin, M.C., Chu, C.J., Tsai, L.C., Lin, H.Y., Wu, C.S., Wu, Y.P., Wu, Y.N., Shieh, D.B., Su, Y.W., Chen, C.D., 2007. Nano Lett. 7, 3656–3661.
Lin, S.P., Pan, C.-Y., Tseng, K.-C., Lin, M.-C., Chen, C.-D., Tsai, C.-C., Yu, S.-H., Sun, Y.-C., Lin, T.-W., Chen, Y.-T., 2009. Nano Today 4, 235–243.
Lin, S.-Y., Liu, S.-W., Lin, C.-M., Chen, C.-H., 2002. Anal. Chem. 74, 330–335.
Lin, T.W., Hsieh, P.J., Lin, C.L., Fang, Y.Y., Yang, J.X., Tasi, C.C., Chiang, P.L., Pan, C.Y., Chen, Y.T., 2010. Proc. Natl. Acad. Sci. U.S.A. 107, 1047–1052.
MacDonald, P.E., Ha, X.F., Wang, J., Smukler, S.R., Sun, A.M., Gaisano, H.Y., Salapatek, A.M., Backx, P.H., Wheeler, M.B., 2001. Mol. Endocrinol. 15, 1423–1435.
Mcalpine, M.C., Agnew, H.D., Rohde, R.D., Blanco, M., Ahmad, H., Stuparu, A.D., Goddard, W.A., Heath, J.R., 2008. J. Am. Chem. Soc. 130, 9583–9589.
Meuwis, K., Boens, N., De Schryver, F.C., Gallay, J., Vincent, M., 1995. Biophys. J. 68, 2469–2473.
Nagatoishi, S., Nojima, T., Juskowiak, B., Takenaka, S., 2005. Angew. Chem. 117, 5195–5198.
Nooney, J.M., Peters, J.A., Lambert, J.J., 1992. J. Physiol. 455, 503–527.
Ohno, Y., Maehashi, K., Yamashiro, Y., Matsumoto, K., 2009. Nano Lett. 9, 3318–3322.
Pan, C.-Y., Lee, H., Chen, C.-L., 2006. Neuropharmacology 51, 18–26.
Pan, C.-Y., Wu, A.Z., Chen, Y.-T., 2007. J. Neurochem. 102, 944–956.
Pandey, P.C., Prakash, R., 1998. Sens. Actuators B 46, 61–65.
Patolsky, F., Timko, B.P., Yu, G., Fang, Y., Greytak, A.B., Zheng, G., Lieber, C.M., 2006. Science 313, 1100–1104.
Patolsky, F., Zheng, G., Hayden, O., Lakadamyali, M., Zhuang, X., Lieber, C.M., 2004. Proc. Natl. Acad. Sci. U.S.A. 101, 14017–14022.
Pui, T.-S., Agarwal, A., Ye, F., Huang, Y., Chen, P., 2011. Biosens. Bioelectron. 26, 2746–2750.
Raymo, F.M., Yildiz, I., 2007. Phys. Chem. Chem. Phys. 9, 2036–2043.
Rose, M.C., Henkens, R.W., 1974. Biochim. Biophys. Acta 372, 426–435.
Rosi, N.L., Mirkin, C.A., 2005. Chem. Rev. 105, 1547–1562.
Sala, F., Nistri, A., Criado, M., 2008. Acta Physiol. 192, 203–212.
Shan, C., Yang, H., Song, J., Han, D., Ivaska, A., Niu, L., 2009. Anal. Chem. 81, 2378–2382.
Singh, N.A., Charlier, C., Stauffer, D., DuPont, B.R., Leach, R.J., Melis, R., Ronen, G.M., Bjerre, I., Quattlebaum, T., Murphy, J.V., McHarg, M.L., Gagnon, D., Rosales, T.O., Peiffer, A., Anderson, V.E., Leppert, M., 1998. Nat. Genet. 18, 25–29.
Star, A., Gabriel, J.-C.P., Bradley, K., Gruner, G., 2003. Nano Lett. 3, 459–463.
Steed, J.W., Atood, J.L., 2000. Supramolecular Chemistry. Chichester, New York.
Stern, E., Steenblock, E.R., Reed, M.A., Fahmy, T.M., 2008. Nano Lett. 8, 3310–3314.
Tansil, N.C., Gao, Z.Q., 2006. Nano Today 1, 28–37.
Tian, B., Cohen-Karni, T., Qing, Q., Duan, X., Xie, P., Lieber, C.M., 2010. Science 329, 830–834.
Tsai, C.-C., Yang, C.-C., Shih, P.-Y., Wu, C.-S., Chen, C.-D., Pan, C.-Y., Chen, Y.-T., 2008. J. Phys. Chem. B 112, 9165–9173.
Varma, S., Sabo, D., Rempe, S.B., 2008. J. Mol. Biol. 376, 13–22.
Vassanelli, S., Fromherz, P., 1999. J. Neurosci. 19, 6767–6773.
Wang, C.-W., Pan, C.-Y., Wu, H.-C., Shih, P.-Y., Tsai, C.-C., Liao, K.-T., Lu, L.-L., Hsieh, W.-H., Chen, C.-D., Chen, Y.-T., 2007. Small 3, 1350–1355.
Wrobel, G., Seifert, R., Ingebrandt, S., Enderlein, J., Ecken, H., Baumann, A., Benjamin Kaupp, U., Offenhausser, A., 2005. Biophys. J. 89, 3628–3638.
Xiao, Y., Meyer, E.L., Thompson, J.M., Surin, A., Wroblewski, J., Kellar, K.J., 1998. Mol. Pharmacol. 54, 322–333.
Xu, J., Wang, X., Ensign, B., Li, M., Wu, L., Guia, A., Xu, J., 2001. Drug Discov. Today 6, 1278–1287.
Zheng, G.F., Patolsky, F., Cui, Y., Wang, W.U., Lieber, C.M., 2005. Nat. Biotechnol. 23, 1294–1301.